AIAA Guidance, Navigation, and Control Conference and Exhibit
11-14 August 2003, Austin, Texas

AIAA 2003-5727

AN ADAPTIVE APPROACH TO VISION-BASED FORMATION CONTROL

Ramachandra Sattigeri*, Anthony J. Calise†
School of Aerospace Engineering, Georgia Institute of Technology, Atlanta, GA 30332-0150

Johnny H. Evers‡
Munitions Directorate, Air Force Research Laboratory, Eglin AFB, FL 32542-6810

ABSTRACT

In considering the problem of formation control in the deployment of intelligent munitions, it would be highly desirable, both from a mission and a cost perspective, to limit the information that is transmitted between vehicles in formation. However, the lack of information regarding the state of motion of neighboring vehicles can lead to degraded performance and even instability. This paper presents an adaptive output feedback approach for addressing this problem. We design adaptive formation controllers that allow each vehicle in formation to maintain separation and relative orientation with respect to neighboring vehicles, while avoiding obstacles. The method works by enabling each vehicle in the formation to adaptively correct for the effect that the motions of neighboring vehicles have when regulating relative variables like range and line of sight. It is assumed that estimates of these variables can be derived using passive, vision-based sensors. The need for explicit communication to maintain formation is minimized and the resulting controller solution is decentralized. We implement a reactive obstacle avoidance controller to navigate in an environment with obstacles. The formation controller and obstacle avoidance controller are outer-loop controllers whose outputs are speed and heading commands. These commands are blended together to generate composite speed and heading commands that are inputs to the inner-loop controller. The weights used for blending the commands depend upon the priority of the task at hand. We illustrate the method with an example involving a team of three aircraft keeping formation in the presence of obstacles.

INTRODUCTION

As demonstrated in recent conflicts, unmanned aerial vehicles (UAVs) are becoming an important component of our military force structure. UAVs, operating in close proximity to enemy forces, provide real-time information difficult to obtain from other sources, without risk to human pilots. Technology demonstration programs such as UCAV illustrate the trend toward development of UAVs that will dominate enemy airspace through maintenance of a continuous presence over the battlefield. Among the weapons employed by these UAVs will be flocks of cooperative miniature or micro autonomous vehicles (MAVs) operating in close proximity to terrain or structures that will gather information on enemy movements and, under human supervision, seek out, identify, and attack targets of opportunity. Of course, reduction in size must be traded against a concomitant reduction in loiter time due to reduced fuel or battery capacity. In addition to advancements in propulsion technologies, concepts for exploitation of unsteady aerodynamics to reduce drag are being explored. In large groups of MAVs or small UAVs, even small percentage reductions in drag will offer significant increased payoffs in the ability to maintain persistent coverage of a large area. One concept, well known to bicyclists, race car drivers, and pilots and exploited by swimming and flying animals, is the benefit of operating in the wake of another vehicle (or organism). Therefore maintaining a formation while at the same time executing searches in a congested environment will be a primary requirement. Stealth like operations will also be important, implying the need to maintain autonomy and to minimize communication. Maintaining a formation is also important from this perspective so that passive (vision based) sensing can be used to ascertain the locations

* Graduate Research Assistant. gte334x@prism.gatech.edu
† Professor. Fellow AIAA. anthony.calise@ae.gatech.edu
‡ Chief, Autonomous Control Team. Senior Member AIAA. evers@eglin.af.mil

and behaviors of cooperating MAVs/UAVs. Various approaches to close-coupled formation flight control for drag reduction include PID control,[1] linear quadratic regulator (LQR) based decentralized control[2] and an adaptive approach[3]. In this paper, we do not focus on the aerodynamic interaction effects of formation flight. Instead we focus on the coupling of the aircraft kinematics due to their measurement and control strategies. [4] We consider formation control within the context of coordinated group motion.

Although imperfectly understood, flocking behavior of birds, schooling behavior of fish, and even studies of swarming insects have provided inspiration for concepts of coordinated multi-vehicle operation. [5] Existing works on coordinated group motion include a distributed behavioral approach to synthesizing the flocking motion of boids[6] (bird and fish-like objects). This approach assumes a flock is the result of the interaction between the behaviors of individual boids (used here to refer to individual autonomous agents operating in a coordinated manner). It was similarly shown in Ref. 7 that coordinated multi-robot motion could be constructed by using a small *basis* set of behaviors. A control-theoretic approach to formation control is given in Ref. 8. The control laws are derived from input-output feedback linearization theory. [9] The control laws allow each follower vehicle in the formation to regulate range and relative orientation with respect to one leader vehicle, or range with respect to two leader vehicles, or range with respect to a leader vehicle while maintaining safe distance from obstacles. Switching between the control laws leads to changes in formation shape. Related work on formation control includes assignment of feasible formations[10] and moving into formation. [11]

Most of the approaches for formation control assume that a leader (neighbor) vehicle's state of motion is known at least partially to the follower (other neighboring) vehicles. Ref. 3 assumes the leader vehicle's inertial positions are available to the follower vehicles. Ref. 8 assumes that the leader vehicle's velocities and the relative orientations with respect to the follower vehicles are known to the follower vehicles, either by communication or by estimation. Our approach treats these quantities as modeling uncertainties, whose effect on output regulation is to be canceled by the output of an online adaptive neural network (NN). As a result, each vehicle can regulate both the range and relative orientation to a leader and/or neighboring vehicle without knowing the state and control policy of that vehicle. The controller solution for each vehicle is completely decentralized. It is assumed that each vehicle can measure its own speed, heading, line-of-sight (LOS) range and angle to other vehicles. Vision-based sensors have been successfully implemented on ground robots for autonomous navigation.[8, 12] Recent work has also been done on implementing vision-based navigation for unmanned aerial vehicles. [13]

The controller architecture in our approach is based on dynamic model inversion. Each vehicle in formation makes an assumption that the neighboring vehicles are stationary. This assumption leads to inversion errors that are approximated online by a NN. The theory is based on an error observer approach to adaptive output feedback control of uncertain, MIMO systems. [14] This approach is adaptive to both parametric uncertainty and unmodeled dynamics. The need for this approach stems from the fact that, while the relative degree of the regulated LOS variables is known, the degree of the plant dynamics is unknown. This is due to the fact that we seek a decentralized solution, and ignore the fact that the vehicle dynamics are coupled through the regulated LOS variables. It is also due to the fact that we are ignoring the speed and heading dynamics, and employing these variables as control variables.

The method of Pseudo-Control Hedging (PCH) [15,16] is used to protect the adaptive process from actuator limits. It is also used to protect the adaptive process during periods when it is not in complete control of the vehicle. This can occur when priority is temporarily given to obstacle avoidance, and when LOS separations from more than one aircraft are to be simultaneously controlled.

There are numerous approaches to static obstacle avoidance. A popular approach is the Artificial Potential Field Approach. [17] Other approaches include Motion Planning[18] and 'Steer Towards Silhouette Edge'. [19] In this paper we describe and implement the last approach, because this approach is most suitable for application with vision-based sensors.

The organization of the paper is as follows. The next section summarizes the theory for the error observer approach and states the problem formulation for decentralized formation control. Next, we develop the individual vehicle model and the relative kinematics between two vehicles in a formation. The next section describes the inverting control design for formation control. Following this, we describe the static

obstacle avoidance controller. The control strategy obtained by combining the outputs of the two controllers through a blending mechanism enables the vehicles to navigate as a group in an environment with obstacles. We then present and discuss simulation results that illustrate our approach.

ADAPTIVE OUTPUT FEEDBACK APPROACH

Consider the observable nonlinear system described by

$$\begin{aligned} \dot{x} &= f(x,u) \\ y &= g(x) \end{aligned} \tag{1}$$

where $x \in \Omega \subset \Re^n$ are the states of the system, $u, y \in \Re^m$ are the controls and regulated output variables respectively, and $f(\cdot,\cdot), g(\cdot)$ are uncertain functions. Moreover n need not be known.

Assumption 1 The system in (1) satisfies the condition for output feedback linearizability with vector relative degree $[r_1, r_2, \ldots, r_m]^T$, $r = r_1 + r_2 + \ldots r_m \le n$. [20]

Then there exists a mapping that transforms the system into the so-called normal form:

$$\begin{aligned} \dot{\chi} &= f'(\xi, \chi) \\ \dot{\xi}_i^1 &= \xi_i^2 \\ &\vdots \\ \dot{\xi}_i^{r_i} &= h_i(\xi, \chi, u) \\ \xi_i^1 &= y_i, \; i = 1,2,\ldots,m, \end{aligned} \tag{2}$$

where $h_i(\xi, \chi, u) = h_i(x,u)$, where $\xi = [\xi_1^T \ldots \xi_m^T]^T$, $\xi_i = [\xi_i^1 \ldots \xi_i^{r_i}]^T$ and χ are the states associated with the internal dynamics. Note that ξ_i^{j+1} is simply the j^{th} time derivative of y_i.

Assumption 2 The zero dynamics are asymptotically stable.

The objective is to design an output feedback control law that causes $y_i(t)$ to track a smooth bounded reference trajectory $y_{ci}(t)$ with bounded tracking error.

Controller Design and Tracking Error Dynamics

Feedback linearization is achieved by introducing the following inverse

$$u = \hat{h}^{-1}(y, \nu) \tag{3}$$

where

$$\nu = \hat{h}(y,u) \tag{4}$$

is the pseudo-control signal. The pseudo-control signal $\hat{h}(y,u) = [\hat{h}_1(y,u), \ldots, \hat{h}_m(y,u)]^T$ represents an invertible approximation to $h(x,u) = [h_1(x,u), \ldots, h_m(x,u)]^T$ in (2), which is limited to using only the available measurements and control signal. If outputs other than the regulated output are available for feedback, they may also be used in (3) to form the approximate inverse.

Thus the system dynamics, as far as the regulated output variable is concerned, is given by,

$$y^r = \nu + \Delta \tag{5}$$

where

$$\Delta(\xi, \chi, \nu) = h\left(\xi, \chi, \hat{h}^{-1}(y,\nu)\right) - \hat{h}\left(y, \hat{h}^{-1}(y,\nu)\right) \tag{6}$$

is the inversion error that results from the use of (3) in place of an exact state feedback inverse. The pseudo-control is chosen to have the form

$$\nu = y_c^r + \nu_{dc} - \nu_{ad} \tag{7}$$

where y_c^r are generated by stable reference models that define the desired closed-loop behavior, ν_{dc} is the output of a dynamic compensator designed to stabilize the linearized error dynamics, and ν_{ad} is the adaptive component.

From (5) and (7), the error dynamics are given as,

$$\tilde{y}^r = y_c^r - y^r = -\nu_{dc} + \nu_{ad} - \Delta(x,\nu) \tag{8}$$

From (6) and (7) it is seen that Δ depends on ν_{ad} through ν, and (8) shows that ν_{ad} has to be designed to cancel Δ. Therefore the following assumption is

introduced to guarantee existence and uniqueness of a solution for ν_{ad} .

Assumption 3 The map $\nu_{ad} \mapsto \Delta$ is a contraction over the entire input domain of interest. It can be shown that this assumption leads to the following conditions[21]

$$\text{i) } \operatorname{sgn}\left(\frac{\partial h_i}{\partial u_i}\right) = \operatorname{sgn}\left(\frac{\partial \hat{h}_i}{\partial u_i}\right),\ i = 1,2,\ldots,m\ .$$

$$\text{ii) } \left|\frac{\partial \hat{h}_i}{\partial u_i}\right| > \frac{1}{2}\left|\frac{\partial h_i}{\partial u_i}\right| > 0\ ,\ i = 1,2,\ldots,m\ .$$

The first condition requires that the sign of the control effectiveness is modeled correctly and the second places a lower bound on the estimate of the control effectiveness.

Error Observer

It can be shown that the error dynamics in (8) can be written as

$$\dot{E} = \overline{A}E + \overline{B}\left[\nu_{ad} - \Delta\right] \tag{9}$$

where the elements of *E* are made up of $\tilde{y}_i$ and its derivatives up to order $(r_i - 1)$ and the dynamic compensator states. An error observer is designed based on this equation[14], which results in error estimates $\hat{E}$ that are used in the adaptive update law given below.

Approximation of the Inversion Error

The inversion error Δ can be approximated to any desired degree of accuracy by using a Single Hidden Layer Neural Network (SHL NN) with sufficient number of hidden layer neurons, and having the following input vector, [22,23]

$$\bar{x}(t) = \left[1\ \ \bar{\nu}_d^T(t)\ \ \bar{y}_d^T(t)\right]^T \tag{10}$$

where

$$\bar{\nu}_d^T(t) = \left[\nu(t), \nu(t-d), \ldots, \nu(t-(n_1-1)d)\right]^T,$$
$$\bar{y}_d^T(t) = \left[y(t), y(t-d), \ldots, y(t-(n_1-1)d)\right]^T$$

with $n_1 \geq n$. Since n is unknown, a sufficient number of delayed signals are required.

The input-output map of a SHL NN is given by

$$\nu_{ad} = W^T \sigma\left(V^T \bar{x}\right) \tag{11}$$

where σ is the so-called squashing function. The NN is trained online with the adaptive law

$$\begin{aligned} \dot{W} &= -\Gamma_W\left[2\left(\sigma\left(V^T\bar{x}\right) - \sigma'\left(V^T\bar{x}\right)V^T\bar{x}\right)\hat{E}^T P\overline{B} + kW\right] \\ \dot{V} &= -\Gamma_V\left[2\bar{x}\hat{E}^T P\overline{B}W^T\sigma'\left(V^T\bar{x}\right) + kV\right] \end{aligned} \tag{12}$$

where $\sigma'(z) = \operatorname{diag}\left(\frac{\mathrm{d}\sigma_i}{\mathrm{d}z_i}\right)$, *P* is the positive definite solution to the Lyapunov equation $\overline{A}^T P + P\overline{A} + Q = 0$, with *Q*>0, and Γ_W and Γ_V are the adaptation gains. It has been shown that the adaptive law in eq. (12) guarantees (subject to upper and lower bounds on the adaptation gains) that all error signals and the NN weights are uniformly ultimately bounded. [14]

Pseudo-Control Hedging (PCH)

PCH is introduced to protect the adaptive law from effects due to actuator limits (such as rate and position limits), time delays and unmodeled actuator dynamics. [15,16] The main idea behind PCH methodology is to modify the reference command, y_c, in order to prevent the adaptive element from adapting to these actuator characteristics. This is commonly done by generating the command using a reference model for the desired response. The reference model is 'hedged' by an amount equal to the difference between the commanded and an estimate for the achieved pseudo-control. To compute this difference, a measurement or estimate of the actuator position $\hat{u}$ is required. The pseudo-control hedge signal is given by,

$$\nu_{h_i} = \hat{h}_i\left(y, u_{cmd_i}\right) - \hat{h}_i\left(y, \hat{u}_i\right),\ i = 1,2,\ldots,m\ . \tag{13}$$

The PCH signal is then introduced as an additional input to the reference model. If the reference model update *without PCH* is of the form,

$$y_{c_i}^{r_i} = h_{rm_i}\left(y_{c_i}, \dot{y}_{c_i}, \ldots, y_{c_i}^{r_i-1}, y_{cmd_i}\right),$$

where y_{cmd_i} is the external command signal, then the reference model update *with PCH* is set to

$$y_{c_i}^{r_i} = h_{rm_i}\left(y_{c_i}, \dot{y}_{c_i}, \ldots, y_{c_i}^{r_i-1}, y_{cmd_i}\right) - \nu_{h_i} . \quad (14)$$

The instantaneous output of the reference model used to construct the pseudo-control signal remains unchanged and is given by

$$\nu_{rm_i} = h_{rm_i}\left(y_{c_i}, \dot{y}_{c_i}, \ldots, y_{c_i}^{r_i-1}, y_{cmd_i}\right) \quad (15)$$

The block diagram of the MRAC controller architecture with PCH and error observer is given below.

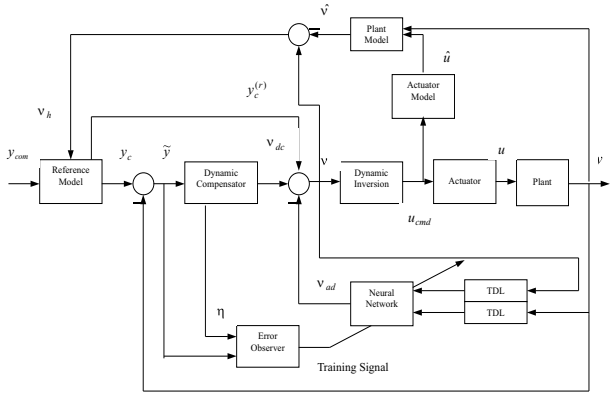

Figure 1. MRAC architecture with PCH

Formation Control Formulation

Consider a group of N vehicles whose individual dynamics are given by,

$$\dot{x}_i = f_i\left(x_i, u_i\right),\ i = 1,2,\ldots,N \quad (16)$$

where x_i represents the states and u_i the control vector of the i^{th} vehicle. Assume that vehicles i and j cooperate by regulating a *joint* variable (e.g., LOS range)

$$z = g\left(x_i, x_j\right) \quad (17)$$

whose relative degree (r) is known, so that,

$$z^{(r)} = g_r\left(x_i, x_{j,} u_i, u_j\right) \quad (18)$$

To arrive at a decentralized control solution, the following approximation is employed by the i^{th} vehicle

$$z_i^{(r)} = \hat{g}_{ri}\left(z, x_i, u_i\right) = \nu_i \quad (19)$$

Equation (19) forms the basis for an inverting control design in which the inversion error is

$$\Delta_i = g_r\left(x_i, x_{j,} u_i, u_j\right) - \hat{g}_{ri}\left(z, x_i, u_i\right) \quad (20)$$

Vehicle $i's$ inverting solution is augmented with a NN that estimates and approximately cancels Δ_i. The input vector to the NN for the i^{th} vehicle is given by $\mu_i = \left[x_i, u_i, \bar{z}_d(t)\right]^T$, where $\bar{z}_d(t)$ is a vector of sufficiently large number of delayed values of $z(t)$ [22,23]. So, the decentralized control solution of all cooperating aircraft is given by $u_i = \hat{g}_{ri}^{-1}\left(\nu_i, z, x_i\right)$, where ν_i is constructed as in equation (7).

APPLICATION TO FORMATION CONTROL

We apply the approach described in the previous section to construct an adaptive formation controller. But first we discuss some modeling issues. The formation of vehicles is constrained to lie in a two-dimensional plane. The vehicles are considered to be point-mass objects that can accelerate both along and perpendicular to the direction of motion. In the following section, the equations of motion for a single vehicle are developed.

Vehicle Dynamics

Consider the equations of motion of an aircraft in the horizontal plane.

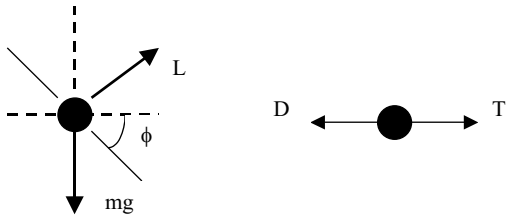

Figure 2. Banked Horizontal Turn

With reference to figure 2, the equations of motion are given by,

$$mV\dot{\psi} = L\sin\phi \tag{21}$$

$$m\dot{V} = T - D \tag{22}$$

$$mg = L\cos\phi \tag{23}$$

where ψ, V represent the heading and speed of the aircraft with respect to an inertial frame that will be specified later, m, ϕ represent the mass and bank angle, L, T, D represent the lift, thrust and drag forces on the aircraft and g is the acceleration due to gravity.

Eliminating ϕ from eqs. (21) and (23),

$$\dot{\psi} = \frac{g}{V}\sqrt{n^2 - 1} \tag{24}$$

$$\dot{V} = \left(\frac{T - D}{W}\right)g \tag{25}$$

where $n = \left(\frac{L}{W}\right)$ is the load-factor of the aircraft. Equations (24) and (25) can be non-dimensionalized by letting $t' = t\left(\frac{V_o}{R_o}\right)$ and $V' = V(V_o)$ represent non-dimensional time and speed, where V_o and R_o are constant quantities with units of speed and distance respectively. A way to choose V_o and R_o would be to set $V_o^2 = gR_o$. Furthermore, we set $V_o = R_o$.
$\Rightarrow V_o = R_o = g$. This implies,

$$\frac{d\psi}{dt'} = \frac{a_1}{V'} \tag{26}$$

$$\frac{dV'}{dt'} = a_2 - \left(\frac{D}{W}\right) \tag{27}$$

where $a_1 = \sqrt{n^2 - 1}$ and $a_2 = \left(\frac{T}{W}\right)$ represent the non-dimensionalized controls. The drag D is given by $D = \frac{1}{2}\rho S V^2 C_D$. The drag coefficient C_D is given by

$$C_D = C_{D_o} + \kappa C_L^2 \tag{28}$$

where C_{D_o} is the profile drag coefficient, assumed to be constant, C_L is the lift coefficient and κC_L^2 = induced drag.

Equation (28) can be modified to replace the lift coefficient with the load factor as follows:

$$n = \frac{L}{W} = \frac{\rho S V^2 C_L}{2W} \Rightarrow C_L = \frac{2nW}{\rho S V^2}.$$

$$\Rightarrow \frac{D}{W} = \left(\frac{\rho S C_{D_o} V_o^2}{2W}\right)V'^2 + \left(\frac{2\kappa W}{\rho S V_o^2}\right)\left(\frac{n^2}{V'^2}\right)$$

$$\frac{D}{W} = k_1 V'^2 + k_2\left(\frac{a_1^2 + 1}{V'^2}\right) \tag{29}$$

where $a_1 = \sqrt{n^2 - 1}$, $k_{1,2}$ are non-dimensional constants and V' is the non-dimensionalized velocity. So the non-dimensional velocity equation is given by substituting for (29) in (27):

$$\frac{dV'}{dt'} = a_2 - k_1 V'^2 - k_2\left(\frac{a_1^2 + 1}{V'^2}\right) \tag{30}$$

Limits on Controls

Since the controls used in our formulation are physical quantities, we need to impose realistic bounds on their values. From (21), (23) and (24), we can write

$$\dot{\psi} = \frac{g}{V}\tan\phi = \frac{g}{V}\sqrt{n^2 - 1}$$

$$\Rightarrow \tan\phi = \sqrt{n^2 - 1} = a_1.$$

If we set the maximum bank angle $\phi_{\max} = 60^o$, we have $n_{\max} = 2$. At low speeds, the maximum load factor is limited by the stall-limit. [24] At low-speeds,

$$n_{\max} = \frac{L_{\max}}{W} = \frac{\rho V^2 S C_{L_{\max}}}{2W} \tag{31}$$

The minimum value of $n_{\max}$ is set to 1 and corresponds to straight, level flight when the lift force equals the weight. The limits for control a_1 are given below,

$$\begin{aligned} a_{1_{\max}} &= \min\left(\tan\phi_{\max}, \sqrt{n_{\max}^2 - 1}\right) \\ a_{1_{\min}} &= \max\left(-\tan\phi_{\max}, -\sqrt{n_{\max}^2 - 1}\right) \end{aligned} \tag{32}$$

The minimum value of $n_{\max}$ is associated with a minimum speed given by

$$V_{\min 1} = \sqrt{\frac{2W}{\rho S C_{L_{\max}}}} \tag{33}$$

At this speed, no turning is possible. A similar method can be used to determine the bounds on a_2. It is assumed that the maximum and minimum values of a_2 do not vary with speed and are equal to ± 0.2. Note that drag equals the maximum value of a_2 at two speeds. The lower of these speeds is set to $V_{\min 2}$. A dynamic lower limit is imposed on a_2 to prevent the speed from going below a minimum value given by

$$V_{\min} = \max(V_{\min 1}, V_{\min 2}) \tag{34}$$

The dynamic lower limit equals the drag force at speeds marginally greater than $V_{\min}$ and switches to equal –0.2 at higher speeds.

We model the actuator system as a saturation element with limits described above

$$u = \text{sat}(u_{cmd}) \tag{35}$$

Relative Kinematics

The kinematics of the i^{th} aircraft in non-dimensional form are given by

$$\dot{x}_i = V_i \cos\psi_i \tag{36}$$

$$\dot{y}_i = V_i \sin\psi_i \tag{37}$$

$$\dot{R}_{ij} = V_j \cos(\psi_j - \lambda_{ij}) - V_i \cos(\psi_i - \lambda_{ij}) \tag{38}$$

$$\dot{\lambda}_{ij} = \frac{V_j \sin(\psi_j - \lambda_{ij}) - V_i \sin(\psi_i - \lambda_{ij})}{R_{ij}} \tag{39}$$

where (x_i, y_i) represent the Cartesian position coordinates of each aircraft with respect to the inertial frame as shown in figure (3). Equations (38) and (39) constitute the relevant kinematical equations for formation flight.

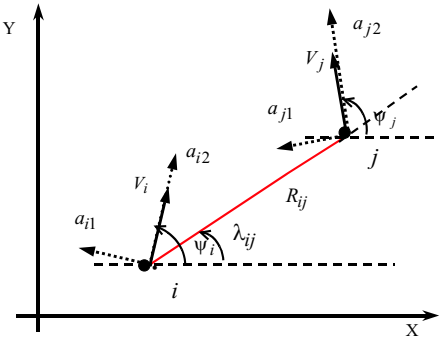

Figure 3. Relative Kinematics

The information available to aircraft *i* include: V_i, ψ_i (by use of an inertial measuring unit IMU), R_{ij}, λ_{ij} (through vision-based sensors) and the control signals a_{i1}, a_{i2}.

Inverting Formation Control Design

We design an inverting controller augmented with a NN for aircraft *i* for regulating the LOS range R_{ij} with respect to aircraft j. The controller architecture is as shown in figure 1. The relative degree of R_{ij} with respect to the speed and heading of aircraft *i* is 1. Hence the range command R_{com} is filtered through a first order reference model. Figure 4 shows the hedged reference model. A rate limit is introduced so that the reference model does not command large range rates when the range error is large. The parameter p is the time constant and is a design parameter.

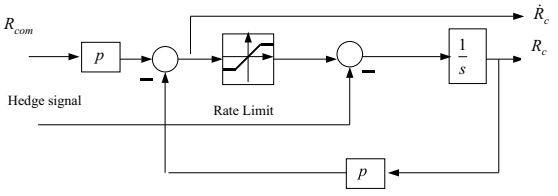

Figure 4. Hedged Reference Model

The dynamic compensator portion of the pseudo-control is a proportional error controller, $\nu_{dc} = k_p\left(R_c - R_{ij}\right)$. The pseudo-control signal is $\hat{\dot{R}}_{ij} = \dot{R}_c + k_p\left(R_c - R_{ij}\right) - \nu_{ad}$.

Equation (38) shows that the LOS range dynamics depends upon the speed and heading of both the vehicles. We assume that aircraft *i* does not know or have access to the state and control policy of aircraft *j*. So, the approximate model used by aircraft *i* for dynamic inversion is given by

$$\hat{\dot{R}}_{ij} = -V_{FCi}\cos\left(\psi_{FCi} - \lambda_{ij}\right) \tag{40}$$

Equation (40) says that aircraft i assumes aircraft j is stationary. An alternate way of assuming an approximate model for aircraft i would be to assume that aircraft j has the same component of speed along and perpendicular to the LOS as aircraft i .

Equation (40) is to be inverted (solved) for the appropriate speed and heading command signals $\left(V_{FCi}, \psi_{FCi}\right)$. This is done as follows. We assume that each vehicle has a body-fixed frame attached to its center of mass. The x-axis of this body frame is always oriented along the direction of the velocity vector. Note that $-\hat{\dot{R}}_{ij}$ represents the commanded velocity vector for aircraft i oriented along the LOS from aircraft i to aircraft j . Figure 5 gives a visualization of the key variables from the perspective of aircraft *i*.

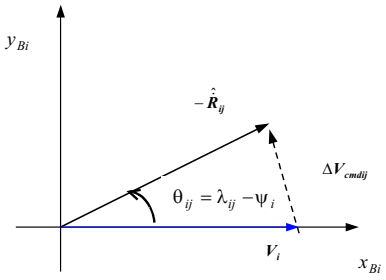

Figure 5. Pseudo-control Vector in Body-Fixed Frame

We write the pseudo-control vector as the sum of its current velocity vector and a perturbation velocity vector. We represent vectors with boldfaced symbols.

$$-\hat{\dot{\boldsymbol{R}}}_{ij} = \boldsymbol{V}_i + \Delta\boldsymbol{V}_{cmdij} = \boldsymbol{V}_{FCi} \tag{41}$$

Here, $\boldsymbol{V}_{FCi}$ represents the velocity vector command for formation control. In case, aircraft i is regulating LOS range with respect to multiple $(N>1)$ aircraft, equation (41) is modified as follows

$$-\sum_{j=1,\, j\neq i}^{N} w_{ij}\ \hat{\dot{\boldsymbol{R}}}_{ij} = \boldsymbol{V}_{FCi} \tag{42}$$

Equation (42) shows that the commanded velocity vector is a weighted average of the pseudo-control vectors associated with multiple neighboring aircraft. The weights w_{ij} are chosen such that $0 \le w_{ij} \le 1$, $\sum_{j=1,\, j\neq i}^{N} w_{ij} = 1$. A simple case results when $w_{ij} = \frac{1}{N}$.

$$\Rightarrow \boldsymbol{V}_{FCi} = -\frac{1}{N}\sum_{j=1,\, j\neq i}^{N} \hat{\dot{\boldsymbol{R}}}_{ij} \tag{43}$$

Equation (43) implies that aircraft i tries to meet the LOS range requirement equally with respect to all the neighboring aircraft. Speed and heading commands are generated from equation (43) as follows:

$$V_{FCi}\cos\theta_{FCi} = -\frac{1}{N}\sum_{j=1,\, j\neq i}^{N} \hat{\dot{R}}_{ij}\cos\theta_{ij}$$

$$V_{FCi}\sin\theta_{FCi} = -\frac{1}{N}\sum_{j=1,\, j\neq i}^{N} \hat{\dot{R}}_{ij}\sin\theta_{ij}$$

where $\theta_{ij} = \lambda_{ij} - \psi_i$. The above equations are solved for $\left(V_{FCi}, \psi_{FCi}\right)$,

$$V_{FCi} = \frac{1}{N}\sqrt{\left(\sum_{j=1,\, j\neq i}^{N} \hat{\dot{R}}_{ij}\cos\theta_{ij}\right)^2 + \left(\sum_{j=1,\, j\neq i}^{N} \hat{\dot{R}}_{ij}\sin\theta_{ij}\right)^2} \tag{44}$$

and $\psi_{FCi} = \psi_i + \theta_{FCi}$ (45)

where $\theta_{FCi} = \tan^{-1}\left(\dfrac{-\sum_{j=1,\, j\neq i}^{N} \hat{\dot{R}}_{ij}\sin\theta_{ij}}{-\sum_{j=1,\, j\neq i}^{N} \hat{\dot{R}}_{ij}\cos\theta_{ij}}\right)$.

Hedge Signals

For the case with adaptation, the reference model for the formation controller in each vehicle is hedged whenever the commanded pseudo-control is not equal to the achieved pseudo-control. The hedge signals for aircraft i are given by

$$\nu_{hij} = \hat{\hat{R}}_{ij} - V_i \cos(\psi_i - \lambda_{ij}) \tag{46}$$

Note that $\nu_{hij} \neq 0$ in three cases:

i) the actuators of aircraft i are saturated,

ii) aircraft i is controlling separation simultaneously from multiple $(N > 1)$ neighboring aircraft and the commanded velocity vector is given by equation (43).

iii) Priority is temporarily given to obstacle avoidance. In this case, $c_1 \neq 0$ (see the next section) and the commanded velocity vector is given by equation (47).

Static Obstacle Avoidance Controller

The controller design strategy for static obstacle avoidance is based on a reactive 'steer towards silhouette edge' approach. [19] The idea is to project the shape of nearby obstacles onto the local, body-fixed frame of the vehicle. If this projected shape, adjusted (enlarged) to allow for the size of the vehicle and the required 'clearance' distance, surrounds the origin of the vehicle's body-fixed frame, then some portion of the obstacle is dead ahead (see figure 6). The vehicle must steer away to avoid a collision, and the most efficient direction to turn is toward that portion of the projected shape that is closest to the origin.

To illustrate the concept, it is assumed that the obstacles are contained within bounding spheres (circles in 2 dimensions), and that the centers (X_o, Y_o) and radii (r) of the obstacles are known. The goal of this strategy is to keep an imaginary line L_o of length D_o, originating at the vehicle's current position and extending in the direction of the velocity vector, from intersecting with any obstacle boundary.[6] The length of this line is typically based upon the vehicle's speed and maneuverability. An obstacle further away than this length D_o is not an immediate threat. The obstacle avoidance behavior considers each obstacle in turn and determines if they intersect with L_o. This intersection calculation is done by checking if (see figure 6)

i) $\text{sgn}(\hat{y}_1) \neq \text{sgn}(\hat{y}_2)$

ii) $\hat{y}_1 = 0$ or $\hat{y}_2 = 0$.

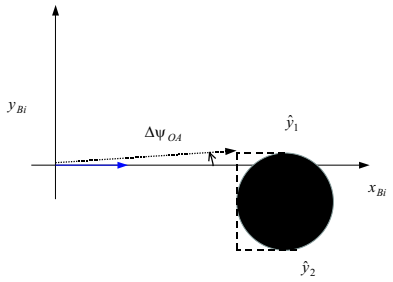

Figure 6. Obstacle Avoidance

If either of the above two conditions is true, then there happens to be a line-obstacle intersection. The obstacle which intersects L_o nearest the aircraft is selected as the "most threatening" and corrective steering action is undertaken to avoid this obstacle. If no obstacle collision is imminent, no steering action is taken.

Note that $\hat{y}_1$ and $\hat{y}_2$ are the extremities of the projected edge of the obstacle in the vehicle's body-frame and are given by $\hat{y}_{1,2} = \hat{Y}_o \pm r$, where $\hat{Y}_o = -(X_o - x_i)\sin\psi_i + (Y_o - y_i)\cos\psi_i$, is the y-coordinate of the center of the obstacle as seen in aircraft i's body-frame.

Corrective steering action to avoid an obstacle involves a speed and heading change command. The heading change command $\Delta\psi_{OA}$ is towards the closest projected edge of the obstacle as shown in figure 6. The speed change command is given by $\Delta V_{OA} = -\dfrac{k_V}{d_{obs}}$, where $d_{obs} = \sqrt{(X_o - x_i)^2 + (Y_o - y_i)^2} - r$ is the distance of the aircraft from the obstacle and $k_V > 0$ is a constant. The speed command for obstacle avoidance is given by $V_{OA} = V + \Delta V_{OA}$.

Composite Speed and Heading Commands

Maintaining a desired formation in the presence of obstacles may not be feasible. However, it is not desirable that each vehicle abandon the group by taking corrective action upon detecting an imminent collision. By blending the commands coming from the obstacle avoidance controller and the formation controller, a compromise between two possibly

conflicting commands can be achieved. The weights used for blending must be chosen carefully in order to guarantee safe and coordinated group motion.
The composite velocity vector command is given by

$$\boldsymbol{V}_{\boldsymbol{cmdi}} = c_1 \boldsymbol{V}_{\boldsymbol{OAi}} + (1-c_1)\boldsymbol{V}_{\boldsymbol{FCi}} \tag{47}$$

which in turn implies the following speed and heading commands

$$\begin{aligned} V_{cmdi} &= \sqrt{V_{Xcmdi}^2 + V_{Ycmdi}^2} \\ \psi_{cmdi} &= \psi_i + \tan^{-1}\left(\frac{V_{Ycmdi}}{V_{Xcmdi}}\right) \end{aligned} \tag{48}$$

where

$$\begin{aligned} V_{Xcmdi} &= \left(c_1 V_{OAi}\cos\Delta\psi_{OAi} + (1-c_1)V_{FCi}\cos\theta_{FCi}\right) \\ V_{Ycmdi} &= \left(c_1 V_{OAi}\sin\Delta\psi_{OAi} + (1-c_1)V_{FCi}\sin\theta_{FCi}\right) \end{aligned} \tag{49}$$

The weight c_1 is chosen to reflect the fact that obstacle avoidance has higher priority than the need for formation keeping. [4]

$$\begin{aligned} &If \;\; d_{obs} \le 3D_o \\ &c_1 = \exp\left(-\left(\frac{d_{obs} - D_o}{D_o^{'}}\right)\right) \\ &else \\ &c1 = 0 \\ &end \end{aligned} \tag{50}$$

$D_o^{'}$ is a scaling factor. Note that $0 \le c_1 \le 1$.

Inner-Loop Controller

The inner-loop controller generates actuator commands to achieve the speed and heading commands.

$$\begin{aligned} a_{i2cmd} &= K_V\left(V_{cmdi} - V_i\right) + k_{i1}V_i^2 + \frac{k_{i2}}{V_i^2}\left(a_{i1}^2 + 1\right) \\ a_{i1cmd} &= K_\psi\left(\psi_{cmdi} - \psi_i\right)V_i \end{aligned} \tag{51}$$

Note that the actuators are subjected to a limit as defined eq. (35), and the discussion that precedes it.

SIMULATIONS

We consider a team of 3 aircraft flying in formation in a 2 dimensional environment with obstacles. Aircraft 1 is the team leader. It sets the trajectory for the formation by commanding a sequence of heading changes at specified time intervals while commanding constant speed. In addition, it also cooperates with the follower aircraft 2 and 3 in regulating desired LOS separation from them. The velocity vector command for the leader aircraft is given by,

$$\boldsymbol{V}_{\boldsymbol{cmd}1} = c_1\boldsymbol{V}_{\boldsymbol{OA}1} + c_2(1-c_1)\boldsymbol{V}_{\boldsymbol{L}1} + (1-c_2(1-c_1))\boldsymbol{V}_{\boldsymbol{FC}1}$$

where $\boldsymbol{V}_{\boldsymbol{L}1}$ refers to the to the leader portion of the total aircraft 1 command. We set $c_2 = 0.7$. Each follower aircraft regulates LOS separation from the leader and from each other. The LOS separations are the jointly regulated variables since the aircraft mutually regulate them to specified values. In addition, the 3 aircraft are also commanded to avoid obstacles during their motion. We present results for cases with adaptation (NN on) and without adaptation (NN off). Hedging is on (H on) only for NN on.

Figure 7 shows the trajectory plot of the maneuver with NN off. The trajectory is marked every 2.5 seconds. Aircraft 1 starts at (0,0), aircraft 2 at (5, -8) and aircraft 3 at (-5, -8). The filled circles represent the obstacles. Figure 8 shows the trajectory plot of the maneuver with NN on. Note that with NN on, aircraft 3 does not go around an obstacle in the first few seconds of the maneuver. This illustrates that adaptation helps the aircraft to make a better choice between formation keeping and obstacle avoidance. Also, note the size of the box that the aircraft fly in figure 8 as compared to figure 7. It is clear that cooperative formation flight is enhanced with NN on.

In figures 9-12 we show results pertaining to aircraft 2. The results for the other aircraft are similar. Figure 9 shows the reference signal tracking with both NN off and NN on. Note that there is significant hedging of the reference command with NN on, and that the tracking is significantly improved in comparison to the NN off result.

Figure 10 shows the control histories for aircraft 2. The controls are frequently saturated during the maneuver. Figure 11 shows the time histories of weight c_1 for aircraft 2. The plot shows that in the first 15 seconds, when the aircraft is near an obstacle, it spends much less time avoiding obstacles with NN on. Figure 12 compares the inversion error with the NN output of aircraft 2.

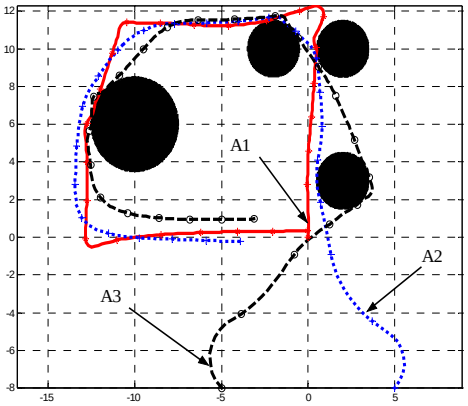

Figure 7. Trajectory (NN off)

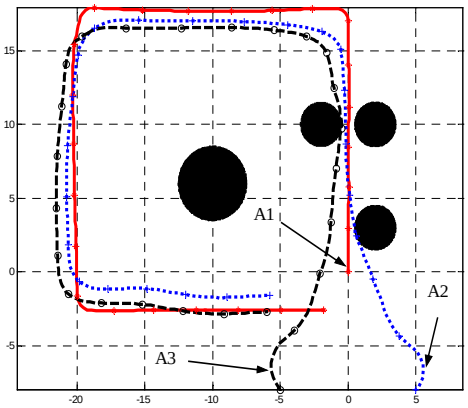

Figure 8. Trajectory (NN on)

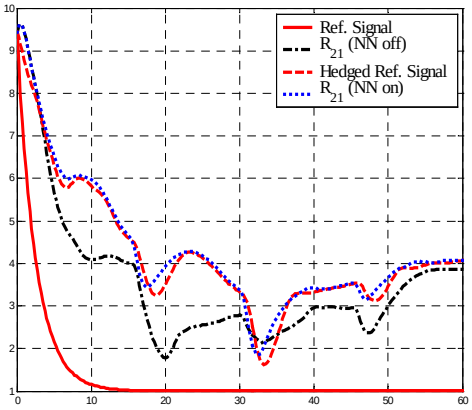

Figure 9. Reference Signal Tracking (Aircraft 2)

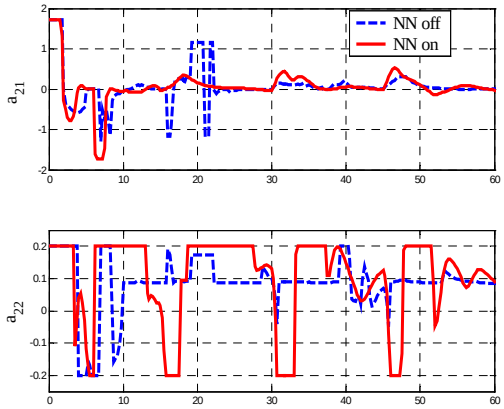

Figure 10. Control Histories (Aircraft 2)

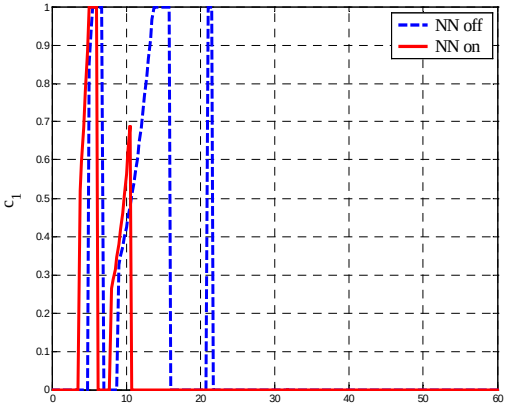

Figure 11. c_1 History (Aircraft 2)

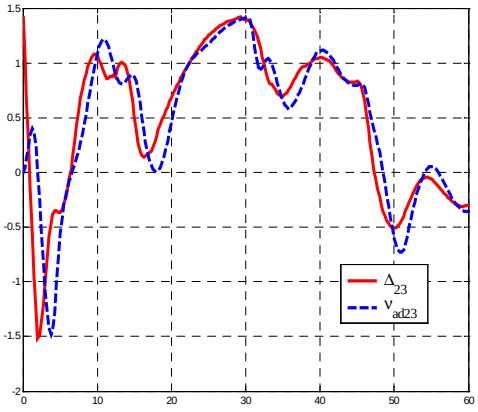

Figure 12. Inversion Error Approximation (Aircraft 2)

CONCLUSIONS

We have formulated a decentralized adaptive guidance strategy that enables safe and coordinated motion of a group of unmanned vehicles in an environment with known obstacles. The strategy blends the outputs of multiple adaptive controllers with a reactive obstacle avoidance controller. There are two key aspects essential to the adaptation process. First, an output feedback formulation is employed that is robust to unmodeled dynamics. Second, pseudo-control hedging is needed to account for actuator saturation, obstacle avoidance and the fact that separations from multiple aircraft cannot be simultaneously controlled. The adaptive controller in each vehicle utilizes local information and LOS measurements obtained with vision-based sensors. This enables each vehicle to correct for the unknown relative motion of neighboring vehicles. The decentralized nature of the controller permits scaling to any number of vehicles in a formation.

ACKNOWLEDGEMENTS

This research has been sponsored under AFOSR contract F4960-01-1-0024 and under NRTC contract NCC 2-945.

REFERENCES

[1]Proud, A., Pachter, M., and D'Azzo, J.J., "Close Formation Control," *AIAA Guidance, Navigation and Control Conference*, Portland, OR, August 1999.

[2]Wolfe, J.D., Chichka, D.F., and Speyer, J.L., "Decentralized Controllers for Unmanned Aerial Vehicle Formation Flight," *AIAA Guidance, Navigation and Control Conference*, San Diego, CA, July 1996.

[3]Schumacher, C.J., and Kumar, R., "Adaptive Control of UAVs in Close-Coupled Formation Flight," *Proc of the American Control Conference*, Chicago, IL, June 2000.

[4]Anderson, M.R., and Robbins, A.C., "Formation Flight as a Cooperative Game," *AIAA Guidance, Navigation and Control Conference*, Reston, VA, August 1998.

[5] Bonabeau, E., Dorigo, M., Theraulaz, G., *Swarm intelligence: from natural to artificial systems*, Oxford University Press, 1999.

[6]Reynolds, C.W., "Flocks, Herds and Schools: a Distributed Behavioral Model," Computer Graphics, 21(4): 71-87,1987.

[7]Mataric, M., *Interaction and Intelligent Behavior*. PhD thesis, MIT, EECS, 1994.

[8]Das, A.V., Fierro, R., Kumar, V., Ostrowski, J.P., Spletzer J., Taylor, C.J., "A Vision-based Formation Control Framework," *IEEE Transactions on Robotics and Automation*, Vol. 18, No. 5, October 2002.

[9]Slotine, J.J., and Li, W., *Applied Nonlinear Control*, Prentice-Hall 1991.

[10]Tabuada, P., Pappas, G., and Lima, P., "Feasible Formations of Multi-Agent Systems," *Proc of the American Control Conference*, Arlington, VA, June 2001, 56-61.

[11]Yamaguchi H., and Arai, T., "Distributed and Autonomous control method for generating shape of multiple mobile robot group," *Proc of the IEEE International Conference on Intelligent Robots and Systems*, Vol 2., 1994, 800-807.

[12]Lorigo, L.M., Brooks, R.A., and Grimson, W.E.L., "Visually-Guided Obstacle Avoidance in Unstructured Environments," *Proc of the IEEE International Conference on Intelligent Robots and Systems*, Vol. 1, 1997, 373-379.

[13]Sinopoli, B., Micheli, M., Donato, G., Koo, T.J., "Vision-based Navigation for an Unmanned Aerial Vehicle," *Proc of the IEEE International Conference on Intelligent Robotics and Automation*, Seoul, Korea, May 2001.

[14]Hovakimyan, N., and Calise, A.J., "Adaptive Output Feedback Control of Uncertain Multi-Input Multi-Output Systems using Single Hidden Layer Networks," *International Journal of Control*, 2002.

[15]Johnson, E., and Calise, A.J., "Feedback Linearization with Neural Network Augmentation applied to X-33 Attitude Control," *AIAA Guidance, Navigation and Control Conference*, Denver, CO, August 2000.

[16]Johnson, E., and Calise, A.J., "Neural Network Adaptive Control of Systems with Input Saturation," *Proc of the American Control Conference*, Arlington, VA, June 2001.

[17]Khatib, O., "Real-Time Obstacle Avoidance for Manipulators and Mobile Robots," *International Journal of Robotics Research*, 1986.

[18]E. Frazzoli, M. Dahleh, "Real-time Motion Planning for Agile Autonomous Vehicles," *Proc of the American Control Conference*, 2001.

[19]Craig Reynolds, "Not Bumping Into Things," *Notes on "obstacle avoidance" for the course on Physically Based Modeling at SIGGRAPH 88*. Available online @ http://www.red3d.com/cwr/nobump/nobump.html

[20]Isidori, A., *Nonlinear Control Systems*, Springer, 1995.

[21]Calise, A.J., Hovakimyan, N., and Idan, M., "Adaptive Output Feedback Control of Nonlinear Systems using Neural Networks," *Automatica*, Vol. 37, No. 8, August 2001.

[22]Hovakimyan, N., Lee, H., and Calise, A.J., "On approximate NN realization of an unknown dynamic system from its input-output history," *Proc of the American Control Conference*, Chicago, IL, June 2000.

[23]Lavretsky, E., Hovakimyan, N., and Calise, A.J, "Upper Bounds for Approximation of Continuous-Time Dynamics Using Delayed Outputs and Feedforward Neural Networks," *IEEE Transactions on Automatic Control*, 2002.

[24]Anderson, J.D., *Introduction to Flight*, McGraw-Hill, 4th Edition, 1999.